

# Out-of-Plane, High strength, Polymer Microneedles for Transdermal Drug Delivery

Buddhadev Paul Chaudhri, F. Ceyskens, H. Pereira Neves, A. La Manna, C. Van Hoof, and R. Puers

**Abstract**—This paper reports on the high strength of high-aspect ratio ( $> 50$ ) hollow, polymer microneedles fabricated out-of-plane using a fairly repeatable fabrication process. Further, these microneedle tips were sharpened by a molding principle, with a simple anisotropic etch of silicon wafer. Also, an enhanced elegant process was explored to incorporate the mounting of the microneedle onto a platform without using any additional material, such that the bore of the microneedle is continuous with the bore of the platform in order to facilitate microfluidic delivery through the hollow needles. The high aspect ratio microneedles undergo failure at the critical load of around 4 N, while the insertion force for such a needle into agar gel, which is a fairly good equivalent of the human skin due to its inherent visco-elastic properties, is 7 mN, which translates into a safety factor (ratio of critical loading force to the maximum applied force) of greater than 500 thus, making it adequately strong for skin penetration.

## I. INTRODUCTION

TRANSDERMAL drug delivery is a particularly an attractive route for delivery of drugs as it by-passes the gastro-intestinal (GI) tract path taken by the conventional oral drug delivery systems. Protein drugs, especially, hormonal drugs cannot be ingested orally as they get digested in the GI tract. Transdermal drug delivery is thus, the delivery of drugs through the skin or sub-dermally directly into the blood stream from where they are circulated inside the body. Though several methods of transdermal drug delivery are in vogue, microneedles score a significant advantage over the other competing technologies in that they are not limited by the size of the drug molecule to be delivered. Also, the length of the needle can be designed to

Buddhadev P. Chaudhri is with the Interuniversity Microelectronics Center (IMEC), Kapeldreef 75, 3001 Leuven, Belgium (phone: +32 16 28 1022, fax: +32 16 28 1576, e-mail: buddha@imec.be) and also with the Division of Microelectronics and Sensors (MICAS), Dept. of Electrical Engineering (ESAT), Katholieke Universiteit Leuven, Arenberg 10, B-3001 Heverlee, Belgium.

F. Ceyskens is with the Division of Microelectronics and Sensors (MICAS), Dept. of Electrical Engineering (ESAT), Katholieke Universiteit Leuven Arenberg 10, B-3001 Heverlee, Belgium.

H. Pereira Neves Hoof is with the Interuniversity Microelectronics Center (IMEC), Kapeldreef 75, 3001 Leuven, Belgium.

A. La Manna is with the Interuniversity Microelectronics Center (IMEC), Kapeldreef 75, 3001 Leuven, Belgium.

C. Van Hoof is with the Interuniversity Microelectronics Center (IMEC), Kapeldreef 75, 3001 Leuven, Belgium and also with the Katholieke Universiteit Leuven, Arenberg 10, B-3001 Heverlee, Belgium.

R. Puers is with the Division Microelectronics and Sensors (MICAS), Dept. of Electrical Engineering (ESAT), Katholieke Universiteit Leuven, Arenberg 10, B-3001 Heverlee, Belgium and also with IMEC, Kapeldreef 75, 3001 Leuven, Belgium.

be short enough (around 300 to 700  $\mu\text{m}$ ) such that it doesn't come in contact with the nerve endings in the dermis layer of the skin, thus, enabling a painless drug delivery system. Prior art research shows that Si and metals have been used extensively as the material of preference for producing microneedles [1, 2]. The ease of fabrication because of time-tested and robust semiconductor processing technologies have only aided in this. But silicon being fragile, is prone to breakage inside the skin and its biocompatibility still being unproven [3], poses a few risks to being used as the structural material for microneedles. Comparatively, polymers are more biocompatible and its visco-elastic properties lead to more resistance to shear-induced breakage [4, 5]. State-of-the-art work mostly involves high-aspect ratio polymer-based microneedles [6] but not on a monolithically fabricated platform, as is the objective of this work.

## II. MATERIALS AND METHODS

Here an epoxy-based polymer, SU-8 (from MicroChem Inc., US) was used the structural material of the microneedle. SU-8 polymer is used as a photoresist which when exposed to UV radiation, causes it to cross-link and thereby forms the needle structure. As will be seen later, this is how these microneedles are produced out-of-plane, that is, the needles stand vertically with their longitudinal axes perpendicular to the plane of the wafer substrate, and thus, out-of-the-plane of the wafer, as is the content of this present work. The counterpart of this is the in-plane process wherein the microneedle is fabricated along the plane of the wafer, that is, its longitudinal axis lies parallel to the plane of the wafer substrate. The feature sizes were defined by a mask. Microneedles were initially produced by a one-step lithography process. High-aspect ratios ( $> 50$ ) were achieved here. These microneedles were subjected to load tests to determine their maximum critical load bearing strength. Furthermore, the microneedles were also inserted into commercially available agar gel, which serves as an equivalent of the human skin due to its visco-elastic properties [7]. Next, the process was enhanced to sharpen the needle tips. Since these microneedles were fabricated directly on the wafer substrate, its lumens were practically blocked by the substrate itself. Thus, their tops were open but their bottoms were blocked as shown in Fig. 1. This serves no practical purpose and thus, in the next improvement, a process for fabricating these needles on a platform, was developed.

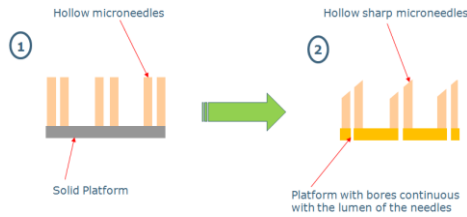


Fig. 1. Schematic of fabricated microneedles. 1 – Hollow non-sharp microneedles, with lumen blocked by the solid platform or the wafer substrate, 2 – Hollow sharp microneedles with an open lumen right through the base platform.

### A. Fabrication - Basic Process

The basic process for the production of the microneedle is fairly simple and is as illustrated in Fig. 2:

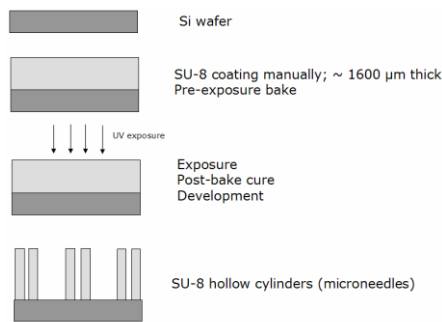


Fig. 2. Basic fabrication process for producing the SU-8 microneedles.

As shown in Fig. 2, a manual coating of SU-8 2050 is applied on the wafer substrate. Because tall microneedles of the order of 1000  $\mu\text{m}$  in height are desired, a thick layer of SU-8 has to be applied. These tall microneedles were designed keeping in mind that they could serve a dual purpose – drug delivery as well as blood extraction. The SU-8 is applied in a dried form: the SU-8 is subjected to a pre-exposure bake at 95°C for 12 hours on a aluminum carrier substrate after which it is broken down into *chips* which are cast on the wafer and heated in a vacuum oven for reflow into an even layer [8], before exposing it to UV for 10 minutes. At this stage, a mask is used to define which region of SU-8 would be exposed to the UV and which regions would be protected. The areas which are exposed get cross-linked and hardened while those which are not, are simply removed in the development stage. After exposure, the SU-8 is subjected to a post-exposure bake at 80°C in an oven, following which it is developed in a developer solution for 30 minutes. During the development the unexposed regions of SU-8 are dissolved and the cross-linked portion emerges prominently, as the SU-8 hollow cylinders, or the microneedles as in Fig. 5.

### B. Fabrication - Enhanced Process

However, it is quite obvious that the microneedles which are fabricated thus with the process illustrated in Fig. 2, though they have a high aspect ratio ( $> 50$ ) as in Fig. 6, and very well defined features, as explained in Fig. 1 above, are

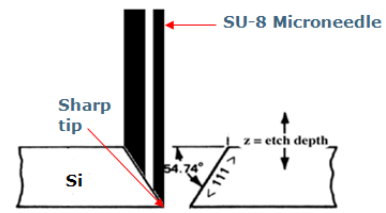


Fig. 3. Principle behind sharpening the microneedle tips by a molding step. Anisotropic etching of a  $\langle 100 \rangle$  Si wafer with KOH causes grooves to be formed along the  $\{111\}$  planes.

substrate not sharp and their lumens are blocked by the wafer on which they stand. Therefore, the above process of Fig. 2 was further augmented by an anisotropic etch step to form sharp-edged pyramidal grooves in the Si wafer using the principle of molding as demonstrated in Fig. 3. Thus, the microneedle is now fabricated with its tip facing downwards as opposed to the earlier process depicted in Fig. 2.

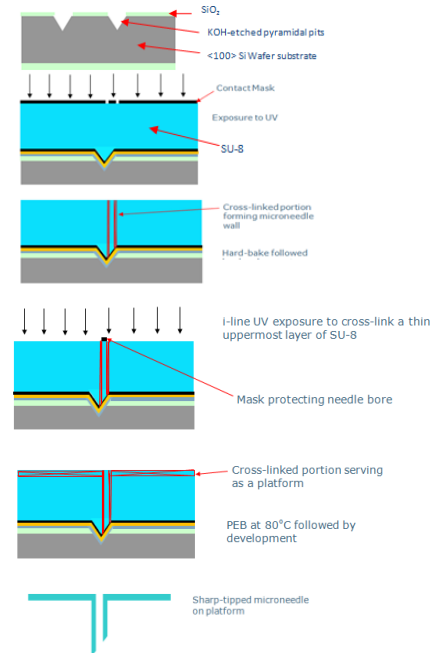


Fig. 4. Fabrication process for producing hollow sharp-tipped microneedles on a platform

It is to be noted here in Fig. 4 that the 54.74° inclined Si plane of the KOH-etched pyramidal pit would reflect the UV light back into the mass of the SU-8, thereby, causing unnecessary cross-linking of the needle lumen resulting in blocking of the same. To prevent this from occurring, an anti-reflective layer of chromium black is coated on the inclined walls of the pyramidal pit. This reduces UV reflectance by 95%. First, a g- and h-line UV radiation is used for the deep exposure of the thick layer of SU-8. Next, the bore of the needle is protected by a mask and then an i-line UV exposure is performed to cross-link only a thin uppermost portion of the SU-8 layer [9], so as to form the platform layer. This is followed by a post-exposure bake at 80°C in an oven, and then developed in developer solution for 30 minutes. Since only the tips of the microneedles are in

contact with the substrate in this process, the resulting adhesive forces between the microneedle tips and the immediate underlying layer of Cr-black are minimal due to the small area of contact. So the microneedle platform arrays are released quite smoothly after the development step. If, however, the platform exposure step is not done, and straightaway a development step is performed, as expected, sharp-hollow needles are formed, but without a platform, as illustrated in Fig. 7.

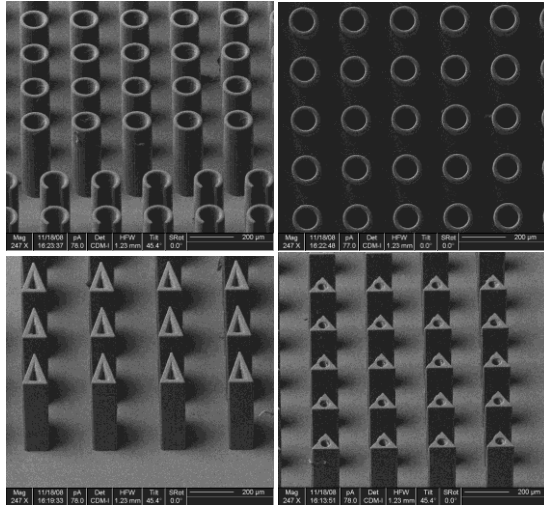


Fig. 5. SEM pictures of short microneedles of 400 µm height of various cross-sections. Top left – Circular cylinders completely round and C-shaped cross-section, Top right – Top view of the same microneedles showing they are hollow inside, Bottom right and left – Triangular cross-sectioned microneedles.

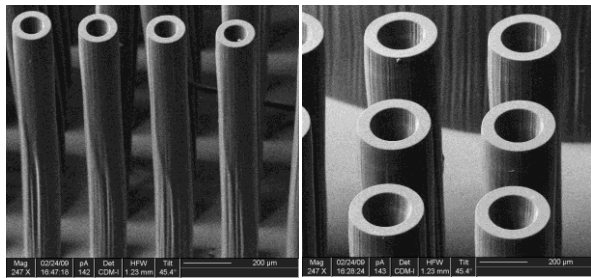


Fig. 6. SEM pictures of fabricated high aspect ratio microneedles. Height: 1540 µm, inner diameter: 100 µm, wall thickness: 30 µm, Aspect ratio: 51.

### III. FABRICATION RESULTS AND DISCUSSION

It is to be noted that Fig. 5 and 6 depict the results of the basic fabrication process as listed in Fig. 2. Here the SU-8 microneedles are observed to be standing on the Si wafer substrate with an achieved aspect ratio of 51. The clear and sharp features of the fabricated microneedles further prove the practical feasibility of such a process. Fig. 7 shows the results of the enhanced fabrication process as denoted in Fig. 4 but as mentioned earlier this was the result of releasing the microneedles without performing the platform exposure step. The tip diameter was measured to be 2 µm, which is considerably sharp as can be seen in Fig. 7 (Right).

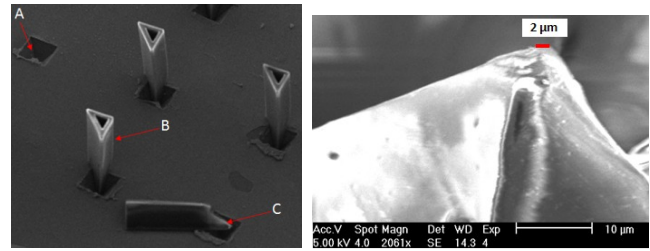


Fig. 7. Left - Sharp-tipped, triangular cross-sectioned microneedles with a triangular cross-sectioned bore: A – KOH-etched pyramidal pit ending at a sharp point, B – a microneedle standing on the pit, C – a fallen microneedle denoting the sharpened tip formed by molding on the pyramidal pit; Right – Close-up of a sharp tip of a microneedle showing the tip diameter of 2 µm.

Thus, the sharp-tipped microneedles are standing on the Cr-black layer on the Si substrate. When the entire enhanced fabrication process of Fig. 4 is completed, microneedles standing out-of-plane on an SU-8 platform, are produced. The fact that no additional material is employed to make the platform plus no extra layer of SU-8 has to be coated onto the existing layer makes the process more attractive and elegant. As can be observed from Fig. 8, the thickness of the platform achieved was about 250 µm which is feasible enough for handling. The height of the microneedles obtained in this case ranged around 600 µm.

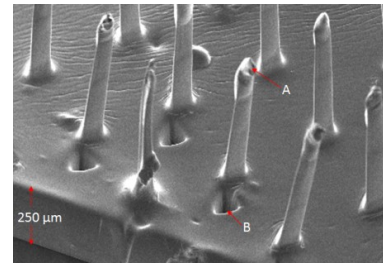


Fig. 8. SU-8 sharp-tipped microneedles fabricated on an SU-8 platform. A – Molded sharp-tips of the triangular cross-sectioned microneedle, B – a bore of the platform misaligned with the bore of the microneedle.

From Fig. 8, it is apparent that misalignment of the bore of the platform presents a considerable challenge, for if the bore is discontinuous with the lumen of the microneedle, the very purpose of the entire process is defeated. The reason why the alignment during the lithography step is even more challenging is because the alignment has to be performed through the very thick layer of SU-8 material already present on the wafer. Work is still on-going in order to optimize this process step.

### IV. MECHANICAL TESTING AND ANALYSIS

The high aspect ratio microneedles fabricated using the basic process flow in Fig. 2, were subjected to a mechanical load testing in order to determine the critical load at which the microneedle fails. For this, an experimental set-up was used wherein a solid metal plunger was orthogonally loaded onto the microneedle top and pressed vertically downwards along the needle axis, manually with the help of a screw

gauge. A force sensor measures the reaction force on the plunger, and so immediately after the point of breakage, the reaction force drops to zero. That point is a measure of the failure force of the microneedle. As can be noted from the graph in Fig. 9, the failure force or the average critical load for the microneedle is 4.18 N for a single hollow microneedle of circular cross-section, height of 1540  $\mu\text{m}$ , inner diameter of 100  $\mu\text{m}$  and a wall thickness of 30  $\mu\text{m}$ .

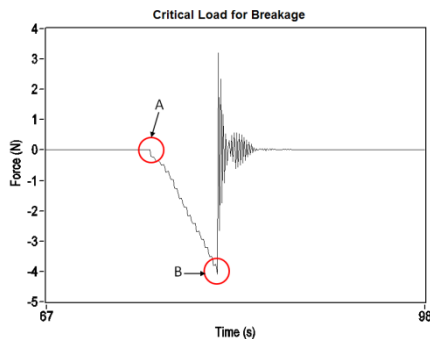


Fig. 9. Average failure force for a single microneedle is measured to be 4.18 N. A – point in time at which the plunger makes contact with the microneedle top, B – point in time at which the microneedle breaks.

To compare this value of the failure force with the insertion force required to insert the microneedles inside the skin, an equivalent model of the skin [6], commercially available agar gel, was utilized. The same above experimental set-up was employed. But now a thin layer of agar gel was placed on top of a (3x3) array of needles or 9 needles in number. Then the plunger was manually moved as before to exert a load on the gel layer, shown in Fig. 10.

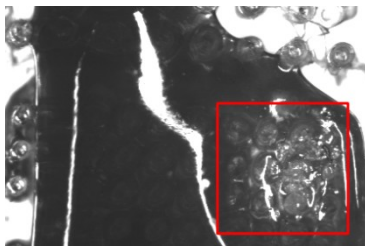


Fig. 10. Actual insertion of the microneedles into agar gel. The dark areas indicate the gel region and the underlying (unpenetrated) microneedles can be observed through the transparent gel. The marked region indicates the area of penetration of an array of (3x3) microneedles into the gel, after being loaded by the plunger.

Peaks in the graph of Fig. 11 are a result of this reaction force of the gel, and the flattening signifies that the microneedles have been completely inserted into the layer of agar gel, thereby exerting no more of the previous elastic reaction force. From the graph in Fig. 11, the insertion force is noted to be 63 mN for the array of (3x3) needles, thus, for a single microneedle the insertion force is computed to be 7 mN. The ratio of the failure force to the insertion force, which is the measure of the safety factor, is therefore, calcu-

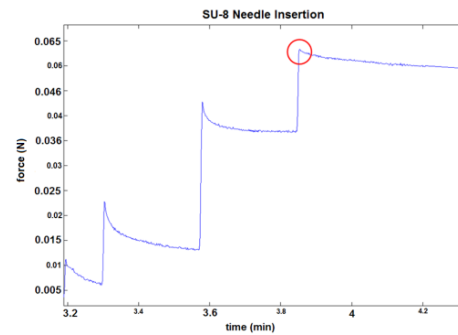


Fig. 11. Applied force on the microneedle as a function of time during the agar gel insertion. Flattening of the peak signifies insertion has just taken place, thereby, indicating an insertion force of 63 mN for an array of (3x3) microneedles.

-lated to be 597, thus, proving the microneedle is sufficiently strong to puncture through such membranes without undergoing failure. Usually mechanical stability and safety mandates a minimum safety factor of 1.5 to 3.

## V. CONCLUSION AND FUTURE WORK

Out-of-plane, polymer microneedles made of SU-8 have been fabricated in various sizes and cross-sections. The strength of the high aspect ratio, polymer microneedles has been proven to be adequate enough to penetrate skin-like membranes without undergoing failure. The process for producing the microneedles on a platform with their bores aligned presents the next formidable challenge. Such microneedles on a platform, thus formed, will have to be tested for mechanical strength and a microfluidic delivery system.

## VI. ACKNOWLEDGEMENT

This work has been funded by IMEC, Belgium and supported thoroughly by ESAT, KU Leuven. The authors are grateful of Tianan Guan of ESAT, KU Leuven, for assisting with the mechanical measurements.

## REFERENCES

- [1] Zahn J D et al 2000 Microfabricated polysilicon microneedles for minimally invasive biomedical devices *Biomed. Microdevices* 2, 295–303
- [2] Stoeber B et al 2000 Two-dimensional arrays out of plane needles ASME Int. Mechanical Engineering Congress and Exposition, MEMS (Orlando, FL)
- [3] Park J-H et al, *J. Control. Release* 104 (2005), 51–66
- [4] Ratner B D et al 1996 *Biomaterials Science: An Introduction to Materials in Medicine* (New York: Academic)
- [5] Wouters K and Puers R 2009 Determining the Young's modulus and creep effects in three different photo-definable epoxies for MEMS applications *Sensors Actuators A*.
- [6] M. Prausnitz, *Advanced Drug Delivery Reviews*, 56, Issue 5, (2004), 581-587
- [7] A. Vexler, I. Polyansky, R. Gorodetsky, *Journal of Investigative Dermatology*, 113 (1999), 732–739
- [8] B. Paul Chaudhri et al, *Journal of Micromechanics and Microengineering*, 20 (2010), 064006
- [9] F. Ceysens, R. Puers, *Journal of Micromechanics and Microengineering*, 16, 2006, pp. S19-S23.